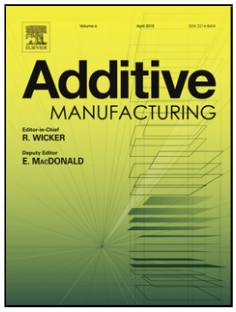

Cork-like Filaments for Additive Manufacturing

S.P. Magalhães da Silva (Conceptualization) (Formal analysis) (Methodology) (Validation) (Investigation)<ce:contributor-role>Data Curation)<ce:contributor-role>Writing - Original Draft)<ce:contributor-role>Writing - Review and Editing), T. Antunes (Investigation) (Formal analysis), M.E.V. Costa (Supervision) (Writing - review and editing) (Funding acquisition), J.M. Oliveira (Conceptualization) (Methodology)<ce:contributor-role>Writing - Review and Editing) (Supervision) (Funding acquisition)

PII: S2214-8604(20)30601-1

DOI: https://doi.org/10.1016/j.addma.2020.101229

Reference: ADDMA 101229

To appear in: *Additive Manufacturing*

Received Date: 12 December 2019

Revised Date: 12 March 2020

Accepted Date: 1 April 2020

Please cite this article as: Magalhães da Silva SP, Antunes T, Costa MEV, Oliveira JM, Cork-like Filaments for Additive Manufacturing, *Additive Manufacturing* (2020), doi: https://doi.org/10.1016/j.addma.2020.101229

Cork-like Filaments for Additive Manufacturing

S. P. Magalhães da Silva [a,b,c*], T. Antunes [c], M. E. V. Costa [c], J. M. Oliveira [a,b,c]

[a] EMaRTGroup – Emerging: Materials, Research, Technology
[b] School of Design, Management and Production Technologies, University of Aveiro, Estrada do Cercal, 449, Santiago de Riba-Ul 3720-509, Oliveira de Azeméis, Portugal
[c] Aveiro Institute of Materials (CICECO), University of Aveiro, Campus Universitário de Santiago, 3810-193 Aveiro, Portugal
[*]Corresponding author: sarapms@ua.pt

Graphical Abstract

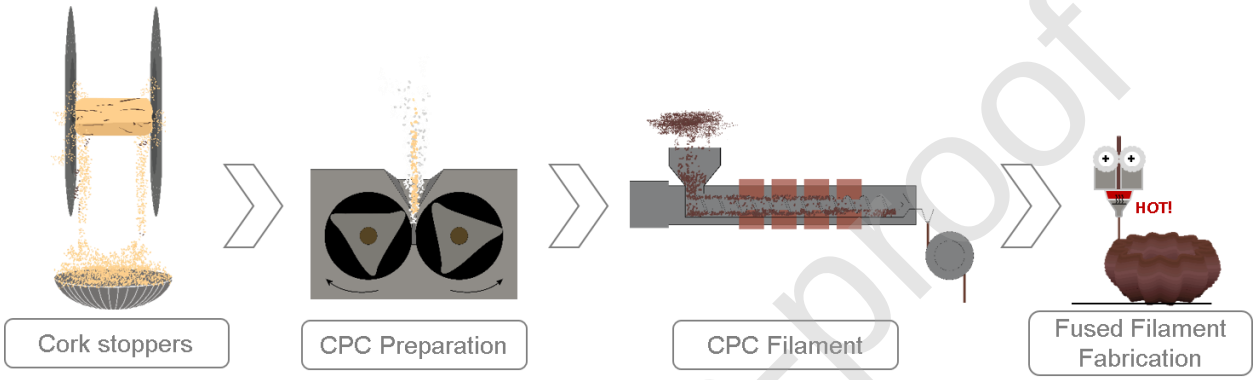

Highlights

- Cork powder residues were used to produce a biodegradable filament for additive manufacturing;
- The addition of a maleic anhydride-based coupling agent to the PLA matrix improved the mechanical behaviour of cork-based composites;
- Printed parts presented a non-plastic and warm touch, along with the release of a pleasant smell during the printing process;

Abstract

A cork-like filament fully biodegradable and filled with low granulometry cork powder residues was developed. Cork-polymer composites (CPC) were prepared using a Brabender type mixer incorporating 15% (w/w) of cork powder (corresponding to 55% (v/v)) and having polylactic acid (PLA) as matrix. In order to promote a chemical adhesion between cork particles and PLA, the effect of maleic anhydride grafted PLA (MAgPLA) was studied. Fourier Transform Infrared – Attenuated Total Reflection (FTIR-ATR) analysis was used to evaluate the functionalization of MAgPLA onto the polymeric chain. The addition of MAgPLA enhanced the mechanical behaviour by increasing tensile properties while improving the dispersion of cork particles within PLA matrix. In addition, cork particles and MAgPLA acted as nucleating agents during PLA melting process. To evaluate the printability of the developed CPC filament, specimens were printed by Fused Filament Fabrication (FFF) and compared to those obtained by injection molding (IM). FFF allowed to preserve the cork alveolar structure in the specimens, benefiting CPC mechanical behaviour. 3D parts could be printed with the CPC filament thereby demonstrating the usefulness of the fully biodegradable cork-based filament here developed. 3D printed parts exhibit unique characteristics, such as a non-plastic and warm touch, a natural colour and the release of a pleasant odour during the printing process.

Keywords

Cork; Composites; Material Extrusion; Additive Manufacturing Coupling agent

1. Introduction

Additive manufacturing (AM) processes involve a set of technologies that produce parts using a layer-by-layer approach. A wide range of materials can be considered for AM, from polymers, metals, ceramics to composite materials. Main advantages of AM are (i) the production of highly customized and also, complex parts without tooling, (ii) a faster product development and manufacturing resulting in a quicker time to market and (iii) on-demand manufacturing by adapting to the market needs [1]. Efforts are being made to change the stigma of AM association to prototyping, with attempts to connect AM to production. Fused Filament Fabrication (FFF) is one of the AM techniques, which builds parts through the extrusion of fused thermoplastic materials. FFF is the most affordable technology with a widespread use, fostered by the development of open-source FFF printers. A lot of effort has been put on the development of a wide range of filament solutions, from low-cost filaments for prototyping/general applications to high-end filaments for technological applications [2–5]. Anisotropy, porosity, layer adhesion and resolution are the main disadvantages when it comes to FFF [6].

Cork is a natural product and Portugal is its main producer in the World. Cork is the outer bark of the Quercus *suber L.* oak tree, which is harvested every 9 years. Owing to its chemical composition, mainly suberin and lignin, and its honeycomb structure composed by closed cells filled with gas, cork has a unique set of properties. Such properties include low density, hydrophobic behaviour, high elastic behaviour and thermal, acoustic and electrical insulation properties [7]. Wine stoppers continue to be the major industrial application of cork. The rectification phase of the cork stoppers production, which involves top- and bottom polishing of stoppers, generates cork powder residues with low granulometries (< 500 μm) [8]. These small cork particles are not used in the development of cork-based products, being usually burned or disposed in landfills. Other well-known cork-based products are insulation boards, wall and floor covering, impact absorption artefacts and aeronautical applications [9–12]. The development of bio-based cork composites for FFF was triggered by the search of new applications for cork and, also by the need to add value to the low granulometry cork powder residues.

Polylactic acid (PLA) is the most abundant biopolymer with properties similar to those of synthetic polymers. It can be found in the market as a biodegradable filament solution. PLA is an aliphatic polyester obtained from ring-opening polymerization of lactide, used as monomer. Lactide results from the depolymerisation of lactic acid obtained by fermentation of sugar from plant-based materials. PLA can be processed by the technologies commonly applied to commercial polymers, such as extrusion, injection moulding, thermoforming and injection blow moulding [13]. However, PLA brittleness, low crystallization rate, hydrophobicity and high cost limit its extended commercialization [14,15]. Within this context, several strategies are being undertaken to overcome these drawbacks, namely the addition of plasticizers [16,17], blending PLA with other synthetic or biodegradable polymers [18,19], addition of reinforcement fillers [20–22] and grafting with compatibilizers [23,24]. The development of sustainable composites with improved thermal and mechanical properties imply the addition of a compatibilizer to improve the interfacial adhesion between the hydrophobic polymeric matrix and the hydrophilic lignocellulosic

fibers. Maleic anhydride (MA) is the most used compatibilizer due to its reactivity and biodegradability [25]. There are several ways to functionalize PLA with MA, being melt functionalization the most applied one [21]. MA grafted PLA (MAgPLA) reacts with hydroxyl groups existing on the surface of natural fibers, creating chemical bonds that bridge polymer and fibers, resulting in composite materials not only with mechanical adhesion but also with improved chemical adhesion between its constituents [21,26]. Numerous studies exploring the development of cork or wood-based 3D printing filaments are found on the literature [4,27–32] and some filaments are already available in the market [33,34]. Kariz *et al.* [4] evaluated the effect of wood content ranging from 0% to 50% (w/w) on the properties of six filaments using PLA as matrix. They concluded that adding more than 10% (w/w) of wood resulted in a decrease of 45% on tensile strength, when compared to pure PLA filaments. Also, as the wood content increases, the surface finishing of printed parts becomes rougher, combined with the presence of voids and wood particle clusters.

The aim of this work was to develop a cork-based and fully biodegradable filament for FFF. Obtaining a filament that exhibits a non-plastic appearance while offering a warm touch after printing was also a goal of this project. This work is part of a continuous research presented elsewhere [35–38]. Thermal, chemical and morphological characterization of the developed cork-polymer composites (CPC) is here assessed. In addition, mechanical and morphological analyses were carried out on injected and printed CPC specimens. The effect of MAgPLA on CPC behaviour was also studied.

Methodology

1.1 Cork

Cork powder residues from a Portuguese cork company were used. The as-received material was fractionated through sieving (Retsch, Germany) using a vibrational sieve shaker. The amplitude used on sieve shaker was 70. Sieves with sizes varying from 200 to 20 µm were used [38]. Particle size distribution (PSD) was determined by measuring the powder mass retained in each sieve and by the design of the cumulative curve, as seen in Fig. 1. The presented values correspond to the average of 3 trials. Through Fig. 1, it is visible that the as-received cork powder presents a bimodal volume distribution over the 40-63 µm and 100-200 range.

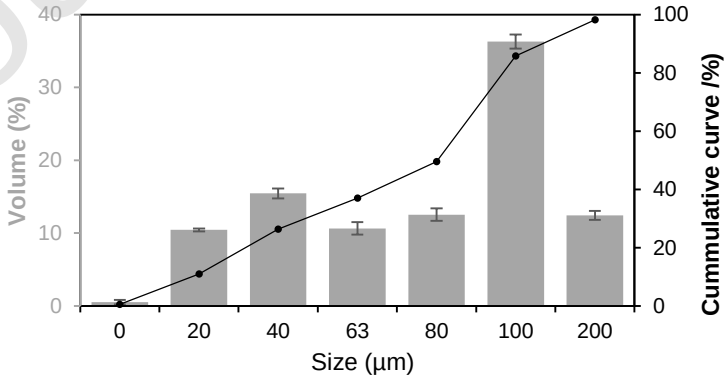

Fig. 1. Particle size distribution of as-received cork powder.

For composites preparation, it was retrieved the cork powder retained in the 40 μm sieve. The average pore diameter as well as the bulk density of this cork powder were determined by mercury intrusion porosimetry (MIP). For that, cork powder was previously dried in a vacuum oven (70 °C) for 24 h. The experiment was conducted in a Micromeritics Auto-pore IV 9500 apparatus. Mercury was then forced to enter into the pores under a pressure ranging from 0.3 MPa to 227 MPa. MIP characterization results of cork powder are presented in Table 1. The reason for the selection of this particle size was related to the typical nozzle size of FFF extrusion system.

1.2 Composites formulation

A PLA with reference 4032D (Ingeo™) from NatureWorks was used and presents a stereoisomer composition of 1.2-1.6 % D-isomer lactide [37,38]. It presents a melting point lying between 155 and 170 °C and a melt flow index (MFI) of 4.60 g/10 min (190°C, 2.16 Kg). The method used for composites formulation is published elsewhere [37,38]. To remove the moisture content, cork powder and PLA were dried at 70 °C during 24h in a vacuum oven (Carbolite AX60 model). In Table 2 are displayed the compositions of the developed CPC. A Brabender type internal mixer was used to prepare the composite materials. The formulation of MAgPLA was also performed by melt functionalization.

Firstly, PLA was charged and melted at 190 °C, during 2 min at 40 rpm, and then cork powder was added and mixed for an additional 8 min. Then, composite materials were granulated into granules (0.5–1.0 mm) using a granulator (Dynisco). The volumetric composition of the final mixture is 45 vol. % of polymeric matrix and 55 vol. % of cork powder, respectively. For CPC 2 preparation, MAgPLA was added together with PLA.

1.3 Thermal analyses

Differential scanning calorimetry (DSC) analysis was employed to evaluate samples thermal behaviour using a Shimadzu DSC-60 equipment. Samples weighing from 8.0 to 10.0 mg were conditioned in aluminium pans and the experiments were carried out in air atmosphere. The temperature profile employed was of 20 to 200°C with a heating rate of 2.5°C/min. The second run was the one considered to determine thermal properties, such as glass transition temperature (T_g), cold crystallization temperature (T_{cc}), melting temperature (T_m), cold crystallization enthalpy (ΔH_{cc}). Melting (ΔH_m) and cold crystallization (ΔH_{cc}) enthalpies were also calculated and the crystallinity degree (X_c) was determined by Eq. 1.

$$X_c = \frac{\Delta H_m - \Delta H_{cc}}{\Delta H_m^0 (1 - w)} \times 100 \qquad (1),$$

where w is the percentage weight of cork and ΔH_m^0 is the melting enthalpy for 100% crystalline PLA (ΔH_m^0 = 93.0 J/g) [39].

1.4 Chemical analyses

Fourier Transform Infrared – Attenuated Total Reflection (FTIR-ATR) measurements were performed in Bruker Tensor apparatus equipped with an ATR golden gate (diamond) from Specac®. Each spectrum was obtained from 256 scans with a 4 cm^{-1} resolution in absorbance mode in the range of 4000-400 cm^{-1}. An average of 3 trails for each sample was considered.

1.5 Mechanical analyses

Mechanical tests were performed using the procedure published elsewhere [37,38]. A universal testing machine Autograph AG-IS (Shimadzu) with a 10kN load cell applying a constant crosshead speed of 1 mm/min was used. Tests were performed at ambient temperature and at least six specimens were tested for each sample. The tensile strength (σ_{max}) and elongation at break (ε_{max}) were taken as the maximum values from the stress-strain curve. Only for comparison purposes, the Young modulus (E) was estimated from the initial slope by linear regression. A micro-injection moulding machine (Babyplast® 610P) was used to prepare the specimens using the conditions presented in Table 3.

Mould cavity was machined considering the preparation of specimens type IV, according to ISO 527-2:1996 standard [40].

1.6 Density

The density (ρ) of samples was determined using an analytic balance (Explorer Pro 210, Ohaus) equipped with a density determination kit (Ohaus, 80253384 model). Distilled water at 25°C was used as immersion medium. For each sample, six measurements were performed being the average value presented here.

1.7 Filament extrusion

CPC 2 filament was prepared using a 3Devo NEXT 1.0 extruder with temperatures ranging from 170 to 190°C [37]. A filament thickness of 1.75 mm was obtained with a tolerance deviation of 5 µm.

1.8 FFF printing conditions

Filaments of PLA and CPC filament were printed into specimens according the standard ISO 527-2:1996 (specimens type IV) [40]. In Fig. 2 is presented the specimens' dimensions and it focuses the applied concentric infill pattern. A Delta WASP 3D printer was used with a 0.4 mm diameter stainless steel nozzle.

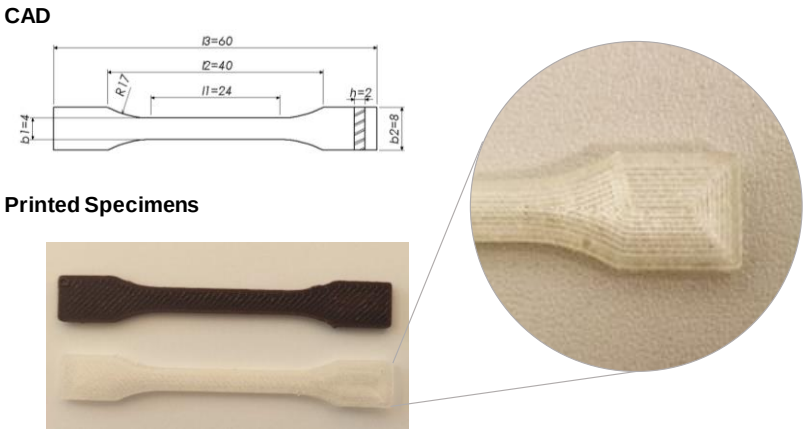

Fig. 2. Specimens' dimensions. The zoom image focuses the concentric infill pattern used.

The printing head was set to 40 mm/s, the nozzle temperature to 190°C and the printing bed temperature to 40°C, for preventing the printed material from warping. It was applied a concentric infill pattern with a layer height of 0.06 mm and an infill percentage of 100%, as published elsewhere [38]. Cura software was used to generate the G-code.

1.9 Morphological analyses

Scanning electron microscopy (SEM) analyses were performed using a SEM Hitachi S4100 equipment. Fracture surfaces obtained after tensile tests of both injected and printed specimens were analysed. The samples were prepared using the methodology published elsewhere [38]. Samples were assembled on aluminium stubs and, then, fixed in a sputter coater chamber (Polaron E 5000). Consequently, to avoid electrostatic charging, samples were sputtered with an Au/Pd target for 2 minutes at 12 mA.

2. Results and Discussion

2.1 Thermal and chemical characterization

DSC melting thermograms of all samples are presented in Fig. 3 and the correspondent thermal parameters are listed in Table 4. PLA exhibited a double melting peaks, while MAgPLA and composites showed a single peak, with T_m values ranging from 150 to 169°C. The lower T_m of PLA in comparison to that of other materials can be attributed to a more cohesive polymeric structure. In addition, the presence of a double-melting peak can be attributed to the occurrence of melting of thinner lamellae followed by the melting of crystals derived from melt-recrystallization [41].

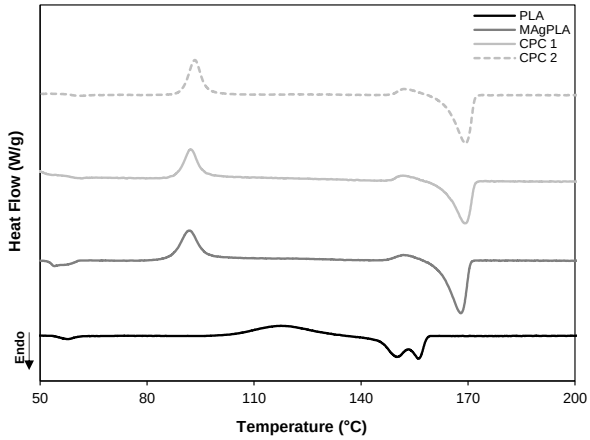

Fig. 3. DSC thermograms of all studied samples.

A shift to lower T_{cc} values occurred when cork was added to the PLA matrix. This is an indication that cork promotes the initial cold crystallization of the PLA matrix due to the heterogeneous nucleation effect. An increase of the crystallinity degree was observed reinforcing the nucleating ability of cork. Also, the presence of MA contributed to the increase of the crystallinity degree of the polymeric matrix. The same tendency was visualized in a previous work performed by Oliveira and co-workers [42].

Fig. 4 presents the FTIR-ATR spectra of all the studied samples. These analyses were made in order to firstly evaluate the grafting of MA onto PLA chain and then to access the interaction of MAgPLA with cork (CPC 2). The characteristic peaks of PLA can be well identified, namely the peak at 1749 cm^{-1}, which is attributed to C=O stretching of PLA ester group. Also the peaks at 1182 cm^{-1} and 1083 cm^{-1}, both related to the C–O bond, are detected [20,43].

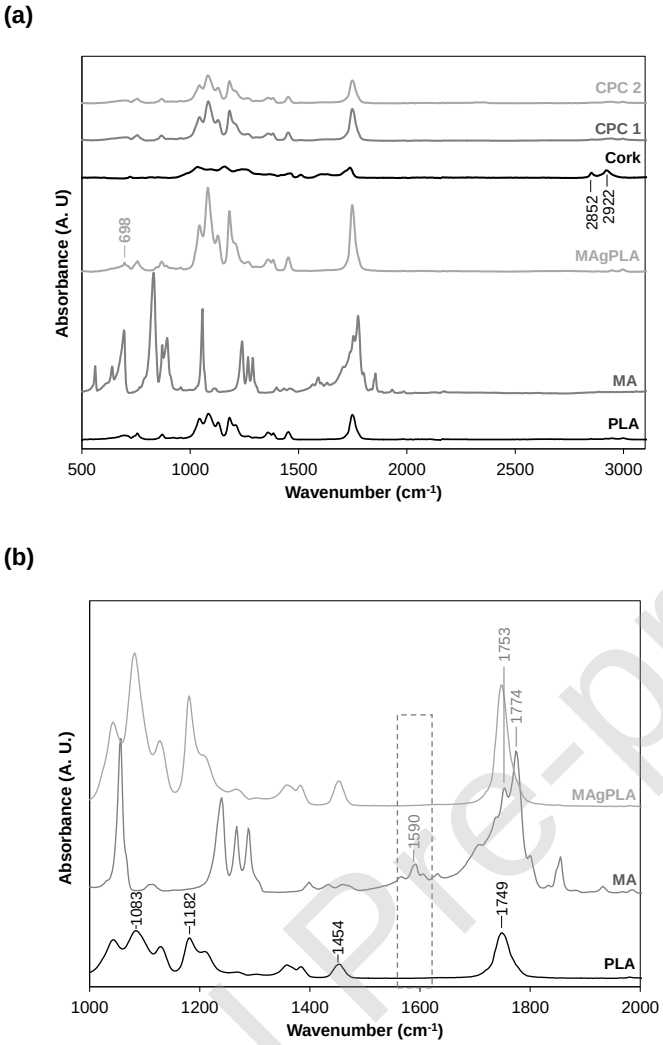

Fig. 4. FTIR-ATR spectra of **(a)** all studied samples and **(b)** zoom-out of PLA, MA and MAgPLA spectra to evidence MA functionalization onto PLA molecular chain.

For MA, it is also visible its distinguishing peaks, such as the peak at 1590 cm^{-1}, which corresponds to the cyclic C=C stretching of anhydride, and the peaks at 1753 and 1774 cm^{-1} associated with the asymmetric stretching of the carbonyl group (C=O) of the cyclic anhydride [21,44]. For MAgPLA spectrum, the absence of the peak at 1590 cm^{-1} is noticed (box delimited area in Fig. 4 (b)) thereby suggesting that MA was grafted onto the PLA chain. The same tendency was observed by Raghu *et al.* [44]. In addition, the presence of the peak at 698 cm^{-1} also indicates that MA was grafted onto the PLA by the bending of the CH group of the anhydride ring [23]. The FTIR-ATR spectrum of cork exhibited the characteristic peaks assigned to suberin, namely the absorption peaks at 2922 cm^{-1} and 2852 cm^{-1} corresponding to asymmetric and symmetric vibrations of C-H, respectively [7]. Vibrations at 1738 cm^{-1} (C=O in suberin), 1159 cm^{-1} (C-O-C ester group in suberin) and 1242 cm^{-1} (C-O stretch in suberin) can also be found. The presence of lignin (guaiacyl) was detected by the vibration peaks at 1510 cm^{-1} and 1463 cm^{-1} [7]. Concerning

the composite materials, the addition of cork to PLA (CPC 1) resulted in a spectrum similar to that of pure PLA (vibration peaks at 1083, 1182 and 1749 cm^{-1}). This can be attributed to the poor interaction between the filler and the polymeric matrix. In the case of CPC 2, those characteristic vibration peaks of PLA shifted to 1081, 1180 and 1747 cm^{-1}, respectively, suggesting that interactions between cork and PLA were improved. In order to perform an accurate analysis without the influence of experimental procedure, these characteristic peaks were normalized by the absorbance peak of PLA at 1454 cm^{-1}. The peak at 1454 cm^{-1} is associated with CH_3 bending vibration, being an internal characteristic peak of PLA [43,45]. In Fig. 5 are displayed the absorbance ratios of pure PLA, MAgPLA, CPC 1 and CPC 2. It is observed that the grafted PLA exhibits a higher intensity of vibration peaks of carbonyl and ether groups due to the presence of MA.

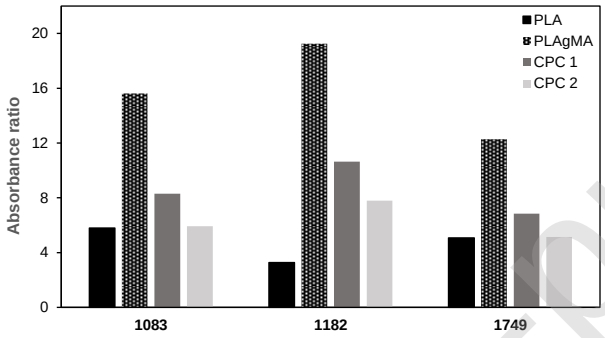

Fig. 5. Absorbance ratio of peaks at 1083, 1182 and 1749 cm^{-1} for pure PLA, MAgPLA, CPC 1 and CPC 2.

Comparing the vibration peak intensities of both composites, the reduced intensity values for CPC 2 can be an indication of an esterification reaction between the hydroxyl groups of cork and MA [21].

2.2 Effect of MAgPLA on CPC mechanical behaviour

The effect of the addition of MAgPLA on the mechanical behaviour of CPC was evaluated. Tensile properties of the developed materials, namely σ_{max}, ε_{max} and Young modulus (E) are presented in Fig. 6.

(a)

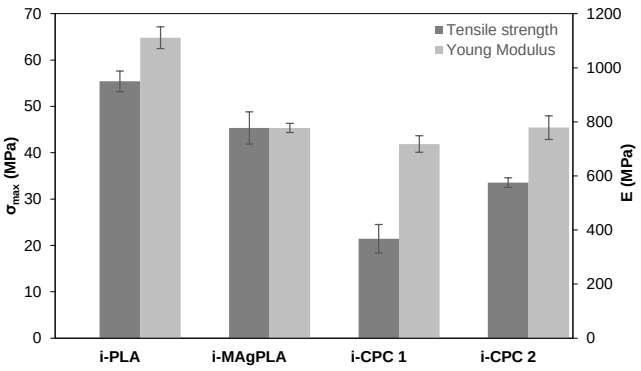

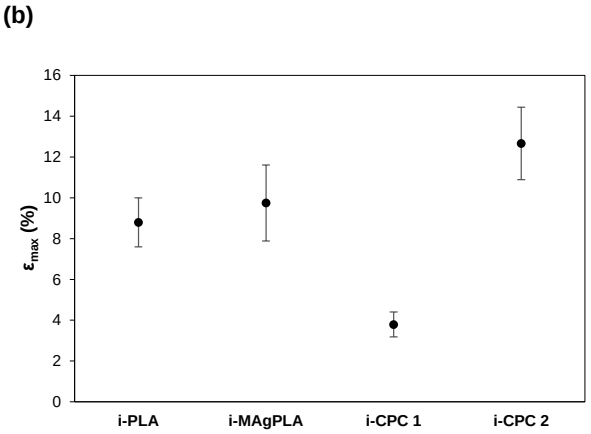

Fig. 6. Mechanical properties of the injected PLA, MAgPLA, CPC 1 and CPC 2: **(a)** tensile strength (σ_{max}) and Young modulus (E); **(b)** elongation at break (ε_{max}). Note: *i* - stands for the injected specimens.

When compared to composites, pure i-PLA exhibits higher tensile strength and modulus. The incorporation of cork into the PLA matrix led to a decrease of ≈61% on the σ_{max} and ≈35% on the Young modulus (i-CPC 1). The decrease on Young modulus can be attributed to the characteristic lower stiffness and foamed structure of cork. Neat PLA is a brittle material and when cork is added to the matrix (i-CPC 1) a decrease of ≈59% on the ε_{max} is noticed. The effect of the high pressure applied during IM process may have an impact on the mechanical properties of composites. Since cork is a cellular material, the high pressure applied will compress the honeycomb structure and the intrinsic cork properties will be damaged. It is known that other mechanisms can also influence the mechanical behaviour of CPC, namely (1) the type of matrix; (2) the compatibility between cork and polymeric matrix; (3) the cork content; and, (4) the dispersion within the matrix and homogenization [37,46]. In order to improve the mechanical behaviour of CPC 1, the effect of a coupling agent to promote the adhesion of cork to PLA was evaluated. To the PLA-Cork system, it was added 4% (w/w) of MAgPLA. The selected amount of MAgPLA was based on previous studies [42,47].

As a result of the addition of MAgPLA to PLA-Cork system, an increase of ≈56% on σ_{max}, of ≈8% on Young modulus and of ≈234% on the ε_{max} were attained. This enhancement of tensile properties can be attributed to the improvement of the interfacial adhesion between the polymeric matrix and cork particles as a result of the establishment of covalent and hydrogen bonds between hydroxyl and anhydride groups. The presence of a coupling agent, such as MA, improves the stress transfer between polymer and filler resulting on the enhancement of composites mechanical behavior. Fig. 6 also shows that MA can act as a plasticizer by reducing σ_{max} and tensile modulus, and by increasing the ε_{max} (i-MAgPLA) [17]. On the other hand, Fourati *et al*. [48] reported an increase of 21% on σ_{max}, of 314% on Young modulus and of 105% on ε_{max} when 2% of MA-based coupling agent was added to a Thermoplastic Starch/Polybutylene Adipate Terephthalate blend.

Several studies on the use of coupling agents in lignocellulosic composites and consequent improvement of mechanical properties are found on the literature. A study from Raghu *et al*. [44]

on the development of thermoplastic starch/PLA blends showed that the presence of 10% of MAgPLA and 20% of wood fiber induced a 86% improvement on σ_{max} and a 106% raise on flexural strength. Fernandes *et al.* [26] reported that the addition of 4 wt.% of polypropylene grafted maleic anhydride promoted an increase of 20% on σ_{max} and of 19% on ε_{max} of CPC. The effect of the same amount of coupling agent showed an increase of 19% on σ_{max} and of 21% on ε_{max} for PLA/Soy protein composites [49]. The mechanical properties of composites are influenced by coupling agents being relevant the following factors: (i) the amount added to the matrix/fiber, (ii) the saturation of the matrix/fiber interface, (iii) the functionalization site and (iv) its functionality [21].

In Fig. 7 are shown SEM micrographs of pure PLA, cork particles and composite materials. PLA exhibited a brittle behaviour reflected on a smooth surface fracture (Fig. 7 (a)). [50]

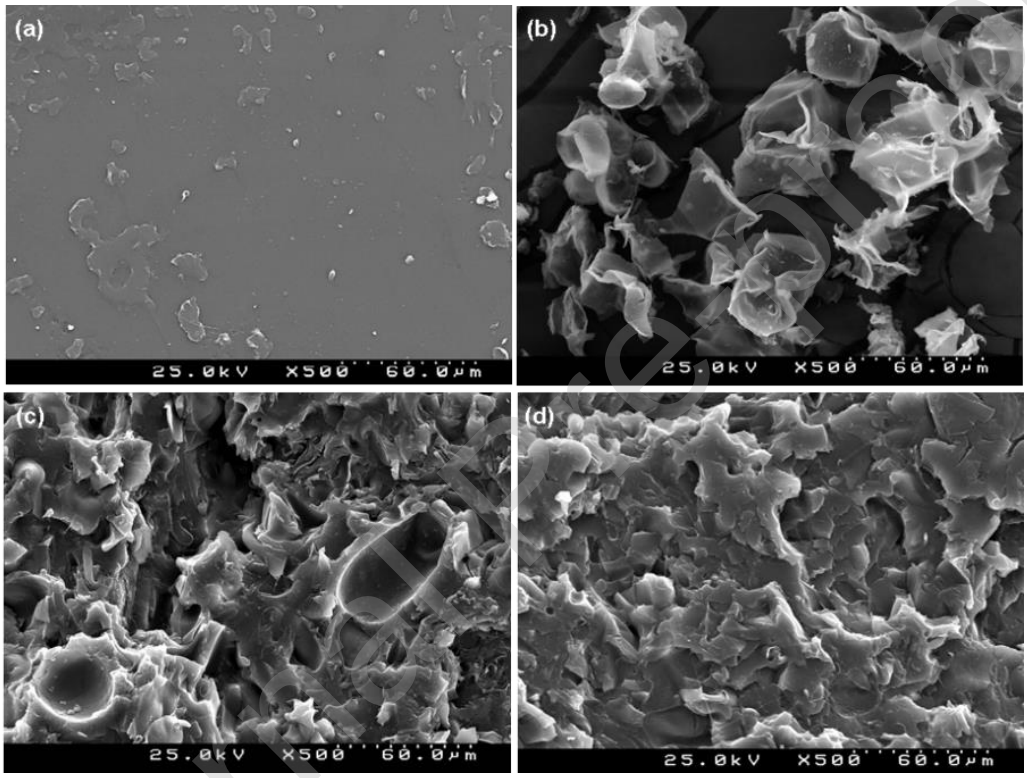

Fig. 7. SEM images of **(a)** pure PLA; **(b)** cork powder; **(c)** i-CPC 1; **(d)** i-CPC 2.

Cork powder residues used in this work came from an industrial polishing process of cork stoppers. In Fig. 7. (b), it is possible to observe that some cork alveolus remain closed, while few of them are damaged as a result of the grinding process. According to Flores *et al.* [51], cork elastic properties are more affected by the content of damaged cells than by their size. This effect on elastic properties is more pronounced for particles smaller than 200 µm. The addition of MAgPLA results on the disappearance of voids and an undetectable interface between cork particles and polymer matrix, as observed when comparing CPC 1 and CPC 2 (Fig. 7 (c)-(d)). SEM micrographs thus reveal that MA acts as a compatibilizing agent by improving the interfacial

adhesion between matrix and filler. These results support those obtained from mechanical analysis.

2.3 Effect of printing conditions on CPC mechanical behaviour

The mechanical behaviour of 3D printed parts should present a behaviour similar to that of parts obtained by conventional methods [52]. Besides manufacturing technologies, the mechanical behaviour of parts is also dependent on the properties of the material itself. For parts printed by FFF the anisotropy acquired during printing is the major problem that is related mainly to the layer size and its consequent thickness. Fig. 8 shows SEM micrographs of a CPC specimen emphasizing the homogeneity and adhesion of printed layers and the average layer height of 60 µm. Printing parameters also influence the mechanical behaviour, such as raster angle, air gap between layers, filament orientation and build direction [52–56]. According to Letcher et al. [55], printed PLA exhibited higher tensile strength for a raster angle of 45°. In addition, a study reported by Chacón et al. [53] showed that samples produced with flat and on-edge orientations had the highest tensile strength and stiffness values. It is important to point out that these were the printing conditions applied in this study.

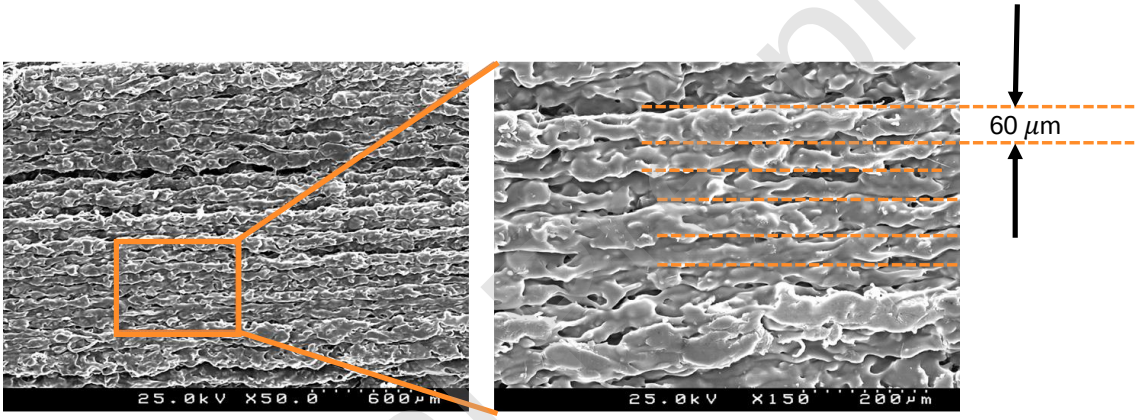

Fig. 8. SEM images of printed CPC specimen highlighting the average layer height.

The mechanical behaviour of printed and injected specimens of PLA and CPC 2 are presented and compared in Fig. 9. As observed, p-PLA sample shows a ≈12% reduction of tensile strength as compared to i-PLA. This reduction can be due to the porosity associated with the FFF process, as can be seen in Fig. 10 (b).

(a)

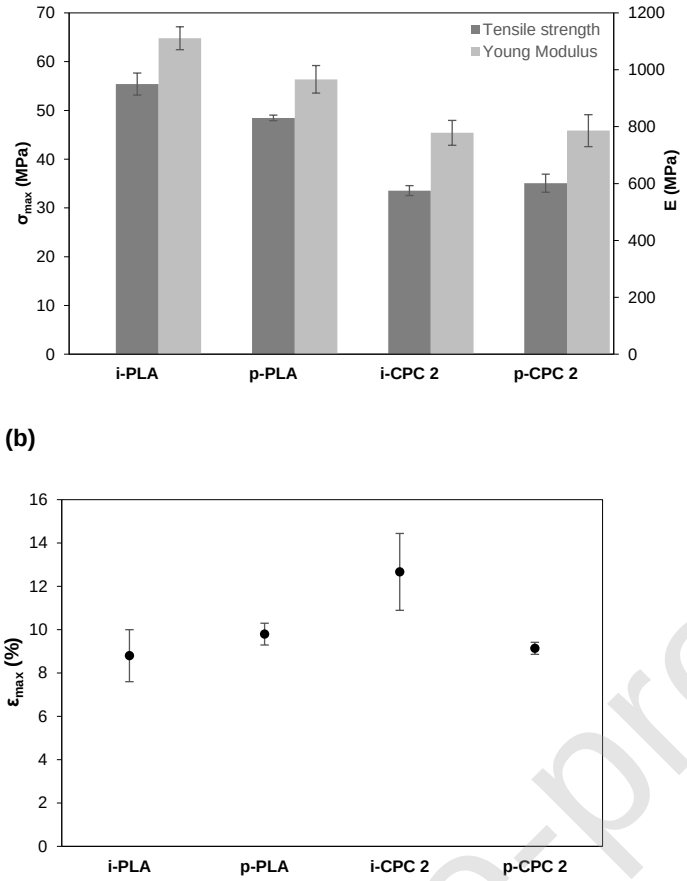

Fig. 9. Mechanical properties of the injected and printed specimens of PLA and CPC 2: **(a)** tensile strength (σ_{max}) and Young modulus (E); **(b)** elongation at break (ε_{max}).

In the case of CPC 2, both injected and printed specimens display similar σ_{max} and E values. The higher ε_{max} value observed for the injected part can be attributed to the rapid cooling down of the molten CPC 2 after the injection process. Contrarily, in the FFF process, CPC 2 is subjected to a longer thermal treatment resulting in a lower cooling rate and, consequently, a higher crystallinity degree. The same tendency was observed by Zhu *et al*. [57], where these differences on the crystallization behaviour resulted in higher σ_{max} and E values and lower ε_{max} values for printed parts, when compared to the IM parts.

SEM micrographs of the injected and printed specimens are presented in Fig. 10. It can be seen that i-CPC 2 and p-CPC 2 specimens exhibit different fracture mechanisms.

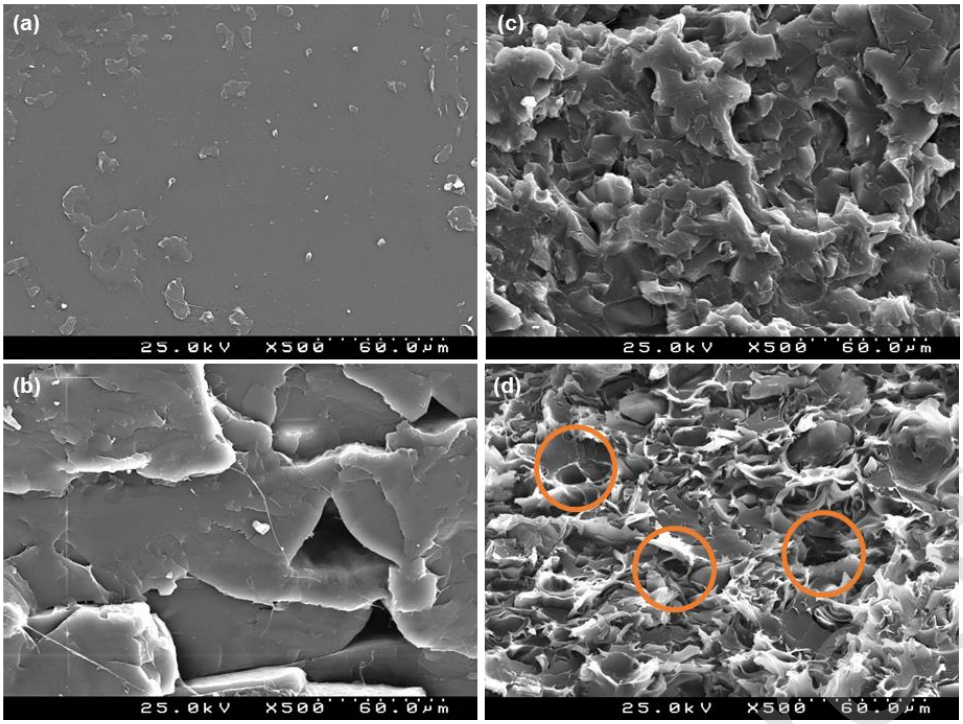

Fig. 10. SEM images of injected and printed specimens: **(a)** i-PLA, **(b)** p-PLA, **(c)** i-CPC 2 and **(d)** p-CPC 2.

i-CPC 2 exhibits a fracture mechanism governed by the matrix while p-CPC 2 shows an intergranular fracture mechanism. The pressures applied during IM and FFF processes have different magnitude, being both processes classified as high- and low-pressure processes, respectively. It is here hypothesized that such different pressures account for the observed distinct fracture mechanisms. This hypothesis is being currently explored (ongoing study).

2.4 Density of injected and printed specimens

In Table 5 the density values for injected and printed specimens are listed. The processing technology and the presence of cork particles affected the density values. As expected, the injected specimens present higher density values than the printed ones. This is due to the higher pressures applied during the injection moulding process as compared to the lower pressures associated to the filament extrusion printing process. The addition of cork did not induce a significant reduction of specimens' density.

This tendency could be associated with the densification of cork particles caused by the pressures applied in both processing methods, also reported by Fernandes *et al*. [46,59]. As it is already known, cork low density is related to its honeycomb structure composed by cells filled with gas. However, in this study, cork powder results from the polishing stage of cork stoppers production, in which the honeycomb cork structure is damaged to some extent. It can be assumed that the contribution of cork particles to the density measurements of composites is associated to the density of cork cell wall, which is estimated to be 1.25 g/cm^3, and also, to the incorporation of PLA into that same damaged cork cells [51].

2.5 Case-study | Printed parts

Fig. 11 shows examples of printed parts using CPC 2 filament. Parts exhibited a non-plastic appearance and a warm touch, similar to that of cork, as well as a smooth surface finishing. An interesting characteristic when using CPC 2 filament is the pleasant smell that is released during the printing process. This is an important feature for desktop printers.

(1)

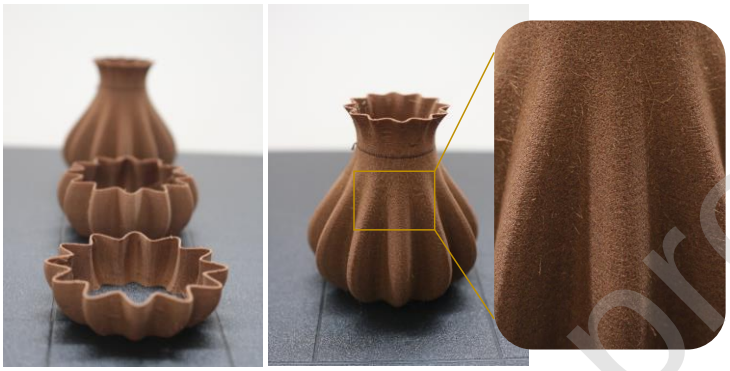

(2)

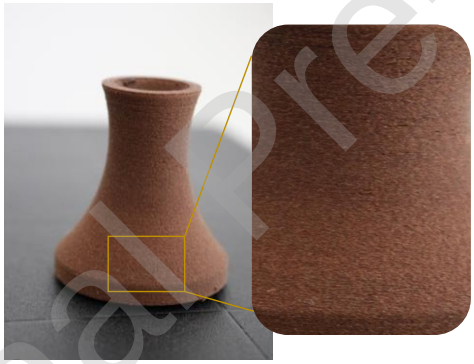

Fig. 11. Examples of printed parts using CPC 2 filament.

The obtained dark-brownish colour is related to the natural colour of cork. The development of CPC filaments presenting new colours solutions is now being conducted.

3. Conclusions

A filament composed by industrial low granulometry cork residues and a biodegradable matrix was developed. The use of these residues on the development of filaments provides a new material solution for AM world with unique characteristics, namely a non-plastic and warm touch, a natural colour and the release of an agreeable odour during the printing process.

PLA was functionalized with MA by a melt functionalization process and the extent of MA grafting was evaluated through FTIR-ATR analyses. The addition of MAgPLA during composite preparation promoted the adhesion and dispersion of cork particles into the polymeric matrix, resulting in an increase of the tensile properties. Both cork and MAgPLA materials acted as

nucleating agents during PLA melting process. The specimens prepared by FFF allowed the cork to preserve its alveolar structure, which benefits CPC mechanical behaviour in opposition to those obtained by IM.

It is here envisaged that the characteristics and properties of this cork-like filament will foster the development of new design solutions and products.

Individual contributions

Sara P. Magalhães da Silva – Conceptualization; Formal analysis; Methodology; Validation; Investigation; Data Curation Writing – Original Draft; Writing – Review & Editing;

Tatiana Antunes – Investigation; Formal analysis;

M. Elisabete V. Costa – Supervision; Writing – Review & Editing; Funding acquisition;

José M. Oliveira – Conceptualization; Methodology; Writing – Review & Editing; Supervision; Funding acquisition;

Acknowledgements

This work was supported by COMPETE 2020 – Programa Operacional Competividade e Internacionalização within TT@ESAN project (NORTE-01-0246-FEDER-000001). This work was also developed within the scope of the project CICECO-Aveiro Institute of Materials, FCT Ref. UID/CTM/50011/2019, financed by national funds through the FCT/MCTES. Authors would also want to acknowledge Maria Celeste Azevedo for the FTIR-ATR measurements and Marta Ferro for the support during SEM analyses.

References

[1] S.A.M. Tofail, E.P. Koumoulos, A. Bandyopadhyay, S. Bose, L. O'Donoghue, C. Charitidis, Additive manufacturing: scientific and technological challenges, market uptake and opportunities, Mater. Today. 21 (2018) 22–37. doi:10.1016/J.MATTOD.2017.07.001.

[2] M.Q. Ansari, M.J. Bortner, D.G. Baird, Generation of Polyphenylene Sulfide Reinforced with a Thermotropic Liquid Crystalline Polymer for Application in Fused Filament Fabrication, Addit. Manuf. 29 (2019) 100814. doi:10.1016/j.addma.2019.100814.

[3] K. Gnanasekarana, T. Heijmans, S. van Bennekomb, H. Woldhuis, S. Wijnia, G. de Witha, et al., 3D printing of CNT- and graphene-based conductive polymer nanocomposites by fused deposition modeling, Appl. Mater. Today. 9 (2017) 21–29.

[4] M. Kariz, M. Sernek, M. Obućina, M.K. Kuzman, Effect of wood content in FDM filament on properties of 3D printed parts, Mater. Today Commun. 14 (2018) 135–140. doi:10.1016/J.MTCOMM.2017.12.016.

[5] B. Brenken, E. Barocio, A. Favaloro, V. Kunc, R.B. Pipes, Fused filament fabrication of fiber-reinforced polymers: A review, Addit. Manuf. (2018). doi:10.1016/j.addma.2018.01.002.

[6] S.C. Ligon, R. Liska, J. Stampfl, M. Gurr, R. Mülhaupt, Polymers for 3D Printing and Customized Additive Manufacturing, Chem. Rev. 117 (2017) 10212–10290. doi:10.1021/acs.chemrev.7b00074.

[7] H. Pereira, Cork : Biology, Production and Uses, Elsevier, Amsterdam, 2007.

[8] L. Gil, Cork powder waste: An overview, Biomass and Bioenergy. 13 (1997) 59–61. doi:10.1016/S0961-9534(97)00033-0.

[9] J.M. Silva, C.Z. Nunes, N. Franco, P. V. Gamboa, Damage tolerant cork based composites for aerospace applications, Aeronaut. J. 115 (2011) 567–575. doi:10.1017/S0001924000006205.

[10] S.P. Silva, M.A. Sabino, E.M. Fernandes, V.M. Correlo, L.F. Boesel, R.L. Reis, Cork: properties, capabilities and applications, Int. Mater. Rev. 50 (2005) 345–365.

[11] F.A.O. Fernandes, R.T. Jardin, A.B. Pereira, R.J. Alves de Sousa, Comparing the mechanical performance of synthetic and natural cellular materials, Mater. Des. 82 (2015) 335–341. doi:10.1016/J.MATDES.2015.06.004.

[12] A.P. Duarte, J.C. Bordado, Cork - A Renewable Raw Material: Forecast of Industrial Potential and Development Priorities, Front. Mater. 2 (2015). doi:10.3389/fmats.2015.00002.

[13] E. Castro-Aguirre, F. Iñiguez-Franco, H. Samsudin, X. Fang, R. Auras, Poly(lactic acid)—Mass production, processing, industrial applications, and end of life, Adv. Drug Deliv. Rev. 107 (2016) 333–366. doi:10.1016/j.addr.2016.03.010.

[14] K. Kamau-Devers, Z. Kortum, S.A. Miller, Hydrothermal aging of bio-based poly(lactic acid) (PLA) wood polymer composites: Studies on sorption behavior, morphology, and heat conductance, Constr. Build. Mater. 214 (2019) 290–302. doi:10.1016/J.CONBUILDMAT.2019.04.098.

[15] E. Vatansever, D. Arslan, M. Nofar, Polylactide cellulose-based nanocomposites, Int. J. Biol. Macromol. 137 (2019) 912–938. doi:10.1016/J.IJBIOMAC.2019.06.205.

[16] A. Carbonell-Verdu, M.D. Samper, D. Garcia-Garcia, L. Sanchez-Nacher, R. Balart, Plasticization effect of epoxidized cottonseed oil (ECSO) on poly(lactic acid), Ind. Crops Prod. 104 (2017) 278–286. doi:10.1016/J.INDCROP.2017.04.050.

[17] S.H. Clasen, C.M.O. Müller, A.T.N. Pires, S.H. Clasen, C.M.O. Müller, A.T.N. Pires, Maleic Anhydride as a Compatibilizer and Plasticizer in TPS/PLA Blends, J. Braz. Chem. Soc. 26 (2015) 1583–1590. doi:10.5935/0103-5053.20150126.

[18] R. Guo, Z. Ren, H. Bi, Y. Song, M. Xu, Effect of toughening agents on the properties of poplar wood

flour/poly (lactic acid) composites fabricated with Fused Deposition Modeling, Eur. Polym. J. 107 (2018) 34–45. doi:10.1016/J.EURPOLYMJ.2018.07.035.

[19] M. Wang, Y. Wu, Y.-D. Li, J.-B. Zeng, Progress in Toughening Poly(Lactic Acid) with Renewable Polymers, Polym. Rev. 57 (2017) 557–593. doi:10.1080/15583724.2017.1287726.

[20] R. Revati, M.S. Abdul Majid, M.J.M. Ridzuan, M. Normahira, N.F. Mohd Nasir, M.N. Rahman Y., et al., Mechanical, thermal and morphological characterisation of 3D porous Pennisetum purpureum/PLA biocomposites scaffold, Mater. Sci. Eng. C. 75 (2017) 752–759. doi:10.1016/j.msec.2017.02.127.

[21] M.E. González-López, J.R. Robledo-Ortíz, R. Manríquez-González, J.A. Silva-Guzmán, A.A. Pérez-Fonseca, Polylactic acid functionalization with maleic anhydride and its use as coupling agent in natural fiber biocomposites: a review, Compos. Interfaces. (2018) 1–24. doi:10.1080/09276440.2018.1439622.

[22] T. Mukherjee, N. Kao, PLA Based Biopolymer Reinforced with Natural Fibre: A Review, J. Polym. Environ. 19 (2011) 714–725. doi:10.1007/s10924-011-0320-6.

[23] S. Detyothin, S.E.M. Selke, R. Narayan, M. Rubino, R. Auras, Reactive functionalization of poly(lactic acid), PLA: Effects of the reactive modifier, initiator and processing conditions on the final grafted maleic anhydride content and molecular weight of PLA, Polym. Degrad. Stab. 98 (2013) 2697–2708. doi:10.1016/J.POLYMDEGRADSTAB.2013.10.001.

[24] S.W. Hwang, S.B. Lee, C.K. Lee, J.Y. Lee, J.K. Shim, S.E.M. Selke, et al., Grafting of maleic anhydride on poly(L-lactic acid). Effects on physical and mechanical properties, Polym. Test. 31 (2012) 333–344. doi:10.1016/J.POLYMERTESTING.2011.12.005.

[25] J.J. Koh, X. Zhang, C. He, Fully biodegradable Poly(lactic acid)/Starch blends: A review of toughening strategies, Int. J. Biol. Macromol. 109 (2018) 99–113. doi:10.1016/J.IJBIOMAC.2017.12.048.

[26] E.M. Fernandes, V.M. Correlo, J.F. Mano, R.L. Reis, Polypropylene-based cork–polymer composites: Processing parameters and properties, Compos. Part B Eng. 66 (2014) 210–223. doi:10.1016/j.compositesb.2014.05.019.

[27] A. Cataldi, D. Rigotti, V.D.H. Nguyen, A. Pegoretti, Polyvinyl alcohol reinforced with crystalline nanocellulose for 3D printing application, Mater. Today Commun. 15 (2018) 236–244. doi:10.1016/j.mtcomm.2018.02.007.

[28] A.M. F.Brites, C. Malça, F.Gaspar, J.F.Horta, M.C. Franco, S. Biscaia, Cork Plastic Composite Optimization for 3D Printing Applications, Procedia Manuf. 12 (2017) 156–165. doi:10.1016/J.PROMFG.2017.08.020.

[29] N. Gama, A. Ferreira, A. Barros-Timmons, 3D printed cork/polyurethane composite foams, Mater. Des. 179 (2019) 107905. doi:10.1016/J.MATDES.2019.107905.

[30] A. Winter, N. Mundigler, J. Holzweber, S. Veigel, U. Müller, A. Kovalcik, et al., Residual wood polymers facilitate compounding of microfibrillated cellulose with poly(lactic acid) for 3D printer filaments, Philos. Trans. R. Soc. A Math. Phys. Eng. Sci. 376 (2018). doi:10.1098/rsta.2017.0046.

[31] M. Tanase-Opedal, E. Espinosa, A. Rodríguez, G. Chinga-Carrasco, Lignin: A Biopolymer from Forestry Biomass for Biocomposites and 3D Printing, Materials (Basel). 12 (2019) 3006. doi:10.3390/ma12183006.

[32] V. Mazzanti, L. Malagutti, F. Mollica, FDM 3D Printing of Polymers Containing Natural Fillers: A Review of their Mechanical Properties, Polymers (Basel). 11 (2019) 1094. doi:10.3390/polym11071094.

[33] ColorFabb, WoodFill, (n.d.). https://colorfabb.com/woodfill (accessed October 29, 2019).

[34] ColorFabb, CorkFill, (n.d.). https://colorfabb.com/corkfill (accessed October 29, 2019).

[35] S.P. Magalhães da Silva, J.M. Oliveira, Cork-Polymer Composites based on Polylatic Acid for Fused Filament Fabrication, in: Mater. 2017, Aveiro, Portugal, 2017.

[36] S.P. Magalhães da Silva, J.M. Oliveira, Green Composites based on Cork Residues for Additive Manufacturing, in: 3rd Int. Conf. Polym. Sci. Eng., Chicago, USA, 2017.

[37] S.P. Magalhães da Silva, J.M. Oliveira, Cork-Polylactide Composites reinforced with Polyhydroxyalkanoates for Additive Manufacturing, in: 18th Eur. Conf. Compos. Mater., Athens, Greece, 2018.

[38] T. Antunes, S.P. Magalhães da Silva, M.E. V Costa, J.M. Oliveira, Cork-based filaments for Additive Manufacturing – The use of cork powder residues from stoppers industry, in: Int. Conf. Addit. Manuf., Maribor, Slovenia, 2018.

[39] E.W. Fischer, H.J. Sterzel, G. Wegner, Investigation of the structure of solution grown crystals of lactide copolymers by means of chemical reactions, Kolloid-Zeitschrift Und Zeitschrift Für Polym. 251 (1973) 980–990.

[40] BS EN ISO 527-2: 1996. Plastics - Determination of tensile properties - Part 2: Test conditions for moulding and extrusion plastics, 1996.

[41] C. Li, Q. Dou, Non-isothermal crystallization kinetics and spherulitic morphology of nucleated poly(lactic acid): Effect of dilithium cis-4-cyclohexene-1,2-dicarboxylate as a novel and efficient nucleating agent, Polym. Adv. Technol. 26 (2015) 376–384. doi:10.1002/pat.3463.

[42] S.P. Magalhães da Silva, P.S. Lima, J.M. Oliveira, Non-isothermal crystallization kinetics of cork-polymer composites for injection molding, J. Appl. Polym. Sci. 133 (2016).

[43] A.A. Cuadri, J.E. Martín-Alfonso, Thermal, thermo-oxidative and thermomechanical degradation of PLA: A comparative study based on rheological, chemical and thermal properties, Polym. Degrad. Stab. 150 (2018) 37–45. doi:10.1016/J.POLYMDEGRADSTAB.2018.02.011.

[44] N. Raghu, A. Kale, A. Raj, P. Aggarwal, S. Chauhan, Mechanical and thermal properties of wood fibers reinforced poly(lactic acid)/thermoplasticized starch composites, J. Appl. Polym. Sci. 135 (2018) 1–10. doi:10.1002/app.46118.

[45] D. Garlotta, A Literature Review of Poly(Lactic Acid), J. Polym. Environ. 9 (2001) 63–84.

[46] E.M. Fernandes, V.M. Correlo, J.F. Mano, R.L. Reis, Cork–polymer biocomposites: Mechanical, structural and thermal properties, Mater. Des. 82 (2015) 282–289.

[47] S.P. Magalhães da Silva, P.S. Lima, J.M. Oliveira, Rheological behaviour of cork-polymer composites for injection moulding, Compos. Part B Eng. 90 (2016). doi:10.1016/j.compositesb.2015.12.015.

[48] Y. Fourati, Q. Tarrés, P. Mutjé, S. Boufi, PBAT/thermoplastic starch blends: Effect of compatibilizers on the rheological, mechanical and morphological properties, Carbohydr. Polym. 199 (2018) 51–57. doi:10.1016/J.CARBPOL.2018.07.008.

[49] R. Zhu, H. Liu, J. Zhang, Compatibilizing effects of maleated poly(lactic acid) (PLA) on properties of PLA/soy protein composites, Ind. Eng. Chem. Res. 51 (2012) 7786–7792. doi:10.1021/ie300118x.

[50] E.M. Fernandes, V.M. Correlo, J.F. Mano, R.L. Reis, Novel cork–polymer composites reinforced with short natural coconut fibres: Effect of fibre loading and coupling agent addition, Compos. Sci. Technol. 78 (2013) 56–62. doi:10.1016/j.compscitech.2013.01.021.

[51] M. Flores, M.E. Rosa, C.Y. Barlow, M.A. Fortes, M.F. Ashby, Properties and uses of consolidated cork dust, J. Mater. Sci. 27 (1992) 5629–5634. doi:10.1007/BF00541634.

[52] J.R.C. Dizon, A.H. Espera, Q. Chen, R.C. Advincula, Mechanical characterization of 3D-printed polymers, Addit. Manuf. 20 (2018) 44–67. doi:10.1016/J.ADDMA.2017.12.002.

[53] J.M. Chacón, M.A. Caminero, E. García-Plaza, P.J. Núñez, Additive manufacturing of PLA structures using fused deposition modelling: Effect of process parameters on mechanical properties and their optimal selection, Mater. Des. 124 (2017) 143–157. doi:10.1016/J.MATDES.2017.03.065.

[54] N. Mohan, P. Senthil, S. Vinodh, N. Jayanth, A review on composite materials and process parameters optimisation for the fused deposition modelling process, Virtual Phys. Prototyp. 12 (2017) 47–59. doi:10.1080/17452759.2016.1274490.

[55] T. Letcher, M. Waytashek, Material Property Testing of 3D-Printed Specimen in PLA on an Entry-Level 3D Printer, in: Vol. 2A Adv. Manuf., ASME, 2014. doi:10.1115/IMECE2014-39379.

[56] I. Durgun, R. Ertan, Experimental investigation of FDM process for improvement of mechanical properties and production cost, Rapid Prototyp. J. 20 (2014) 228–235. doi:10.1108/RPJ-10-2012-0091.

[57] W. Zhu, C. Yan, Y. Shi, S. Wen, J. Liu, Y. Shi, Investigation into mechanical and microstructural properties of polypropylene manufactured by selective laser sintering in comparison with injection molding counterparts, Mater. Des. 82 (2015) 37–45. doi:10.1016/J.MATDES.2015.05.043.

[58] NatureWorks, Ingeo Biopolymer 4032D Technical Data Sheet, n.d. https://www.natureworksllc.com/~/media/Technical_Resources/Technical_Data_Sheets/TechnicalDataSheet_4032D_films_pdf.pdf (accessed March 25, 2019).

[59] E.M. Fernandes, V.M. Correlo, J.F. Mano, R.L. Reis, Polypropylene-based cork–polymer composites: Processing parameters and properties, Compos. Part B Eng. 66 (2014) 210–223. doi:doi.org/10.1016/j.compositesb.2014.05.019.

Table 1. Cork powder characterization by MIP.

Average pore diameter (µm)	23.3
Bulk density (g/cm^3)	0.156
Apparent Density (g/cm^3)	0.694
Porosity (%)	77.6

Table 2. CPC formulation compositions.

Samples	**PLA** (w/w %)	**Cork** (w/w %)	**MAgPLA** (w/w %)
CPC 1	85	15	-
CPC 2	81	15	4

Table 3. Injection moulding conditions.

Temperature profile (°C)	180-185-190
Injection pressure (MPa)	13
Second pressure (MPa)	10

Table 4. Samples thermal parameters obtained from DSC thermograms.

Samples	T_{cc} (°C)	ΔH_{cc} (J/g)	T_m (°C)	ΔH_m (J/g)	X_c **(%)**
PLA	118.3	29.3	150.1; 156.2	-35.9	7.2
MAgPLA	91.9	33.7	168.0	-47.2	14.6
CPC 1	92.7	25.6	169.6	-37.5	15.1
CPC 2	93.4	28.0	169.2	-43.0	19.0

Table 5. Density values for injected and printed specimens – ρ(PLA) equal to 1.24 g/cm^3 [58].

Specimens	**ρ** (g/cm^3)
i-PLA	1.26± 0.01
i-MAgPLA	1.26± 0.02
i-CPC 1	1.22± 0.01
i-CPC 2	1.24± 0.08
p-PLA	1.11± 0.05
p-CPC 2	1.19± 0.02